Int. J. Electrochem. Sci., 8 **(2013)** 10910 - 10920

International Journal of
ELECTROCHEMICAL
SCIENCE
www.electrochemsci.org

Effect of Argon Gas on Photoelectrochemical Characteristics of Film Electrodes Prepared by Thermal Vacuum Evaporation from Synthesized Copper Zinc Tin Selenide

Nordin Sabli[1], *Zainal Abidin Talib*[1,*], *Wan Mahmood Mat Yunus*[1], *Zulkarnain Zainal*[2], *Hikmat S. Hilal*[3], *Masatoshi Fujii*[4]

[1] Department of Physics, Faculty of Science, Universiti Putra Malaysia, 43400 UPM Serdang, Selangor, Malaysia
[2] Department of Chemistry, Faculty of Science, Universiti Putra Malaysia, 43400 UPM Serdang, Selangor, Malaysia
[3] SSERL, Department of Chemistry An-Najah N. University, PO Box 7, Nablus, West Bank, Palestine
[4] Department of Molecular Science, School of Medicine, Shimane University, Izumo, Shimane, 693-8501, Japan
[*]E-mail: zainalat@science.upm.edu.my

Received: 20 May 2013 / *Accepted:* 16 July 2013 / *Published:* 20 August 2013

Copper Zinc Tin Selenide (CZTSe) compound was synthesized from its constituent elements in an evacuated quartz ampoule. The synthesized compound was used as source to deposit film electrodes by vacuum evaporation method under different argon gas flow rates. The argon gas flow rate affected film surface morphology and chemical composition. The film prepared under higher argon gas flow rate of 15 cm^3/min or higher exhibited photoelectrochemically p-type behavior due to the SnSe compound. When using argon flow rate of 10 cm^3/min or lower, the film exhibited mixed p- and n-type behaviors due to mixed CZTSe and ZnSe phases. The deposited films exhibited high absorption coefficient value (> 4.0 x 10^4 cm^{-1}) in the wavelength range of 400 and 800 nm, showing their applicability as visible light energy conversion materials. The results show the potential value of the technique described here, where film electrode main characteristics can be controlled by simply changing the argon gas flow rate.

Keywords: argon gas condensation; thermal evaporation; photoelectrochemical; photoactivity; Copper zinc tin selenide film

1. INTRODUCTION

CZTSe is a semiconductor that is currently being investigated due to its suitability for solar cell applications. CZTSe films can be synthesized using several techniques including vacuum evaporation,

electron beam evaporation, chemical vapour transport and spray pyrolysis [1-8]. Among those techniques, film deposition using vacuum evaporation in the presence of argon gas has its own unique features leading to film shape uniformity, narrow size distribution, and ease of parameter control [9]. The technique has also been effectively used to enhance CZTSe thin film electrodes deposited at room temperature for phoelectrochemical (PEC) applications [10].

CZTSe is a I_2-II-IV-VI_4 chalcogenide semiconductor and has a direct band gap with a high absorption coefficient (> 10^4 cm^{-1}) [10, 11]. Moreover, it involves metal that is with little toxicity and easily available. This can lead to low manufacturing cost and green technology solar cells [12, 13]. CZTSe exhibits a tetragonal structure with lattice parameters of a = b= 5.6880 Å and c = 11.3380 Å [13, 14]. CZTSe films usually possess p-type electrical conductivity; but their electrical properties can be tuned by changing chemical composition.

Since thin film solar cell energy conversion efficiency has not exceeded 20% for the last few decades; scientists have begun looking for new materials for such applications [15, 16]. In this regard, a lot of work has focussed in finding methods to reverse the conductivity type of materials from p-type to n-type and vice versa in order to invent new material properties [17-19]. This work is in parallel with these efforts. CZTSe material, prepared by solid state method with stoichiometric (2:1:1:4) was used as source to deposit films at 100°C substrate temperature using thermal vacuum evaporation in the presence of argon gas for the first time. The effect of argon gas flow rate on resulting film characteristics has been studied.

2. EXPERIMENTAL SECTION

2.1 Chemicals

Pottasium hexacyanoferrate (III), $K_3[Fe(CN)_6]$ and pottasium hexacyanoferrate(II) trihydrate, $K_4[(Fe(CN)_6)].H_2O$ were purchased from Sigma Aldrich. Hydrochloric acid, HCl was purchased from Friendmann Schmidt Chemical. Organic solvents, methanol and 2-propanol, were purchased from Merck KGaA and HmbG Chemicals respectively. Starting materials copper, tin, and selenium were all purchased from Alfa Aesar with nominal purity of 99.8, 99.5 and 99.5% respectively. Zinc was purchased from Nanostructured & Amorphous Materials Inc with nominal purity 99.9%.

2.2 Film electrode preparation

The CZTSe alloy source material was prepared using the melt-quenching method [10]. The mixed powder of copper, zinc, tin and selenium were weighed according to stoichiometric 2:1:1:4 nominal molar ratios, mixed, sealed in a vacuum quartz ampoule and heated. The CZTSe compound was taken out from the ampoules and was ground into fine powder for XRD analysis. The XRD patterns were measured on an XPERT-PRO X-ray diffractometer with Cu K_α [1.54056 Å]. After confirming their structures by XRD, the prepared compounds were then used as source materials.

The prepared CZTSe powder (0.10 g) was placed in a molybdenum evaporation boat. In order to obtain strong adherence and film uniformity, substrates of highly conductive ITO/glass slides, were pre-cleaned prior to deposition. The multi-step cleaning process involved washing with soap, rinsing with distilled water, washing with methanol, rinsing again with distilled water, soaking in dilute HCl 10% (v/v) for 10 s, rinsing with distilled water, washing with methanol, rinsing again with distilled water and rinsing with boiling isopropyl alcohol before drying.

The substrates were mounted on a mask that was placed 14 cm above the boat. The set was then covered with a bell jar and evacuated to a vacuum of 5 X 10^{-4} Pa. A heater was kept directly above the substrate and set at 100°C for every deposition. Thermocouple was used to monitor the temperature substrates. The substrate was heated in order to improve film adhesion, increase surface mobility of condensing atoms and enhance crystallinity [22].

Argon gas was introduced into the vacuum chamber via an inlet tube having a nozzle 0.5 mm in diameter at different flow rate (V_A= 5, 10, 15, 25 cm^3/min). The nozzle was mounted near the evaporation boat, and its outlet direction was pointed towards the substrate. Prior to deposition, the boat containing CZTSe powder was pre-heated for 1 hour at a temperature lower than the melting point (< 900°C). By gradually increasing the applied current, the CZTSe powder melted, evaporated from the boat and deposited on the substrate, which was kept at 100°C during the evaporation process.

Deposited film thickness was measured using an Ambios XP-200 high surface profilometer. The atomic compositions of the as-deposited thin films were investigated by EDX (Oxford Instruments model 7353) attached to a Nova NanoSEM 230 field emission scanning electron microscope (FESEM) which was also used to observe surface morphology. PEC experiments were performed using $[Fe(CN)_6]^{-3}$/$[Fe(CN)_6]^{-4}$ redox system, by running linear sweep voltammetry between +1.0 V and -1.0 V with a scan speed of 20 mV/s using a PGSTAT 101 Potentiostat. A conventional three-electrode cell, equipped with a platinum counter electrode and an Ag/AgCl reference electrode, was used. An Osram halogen lamp was used as a light source. The light intensity at the working electrode was measured to be 0.1 W/cm^2 by a pyranometer (LI-200; Li-Cor, USA) and used to directly illuminate the sample. The light was intermittently chopped at constant frequency to study the effect of photocurrent and dark current.

3. RESULTS AND DISCUSSION

3.1 X-ray diffraction

XRD patterns of the synthesized CZTSe powder are shown in Figure 1. The peaks were well matched with JCPDS Card number 98-006-7242 confirming the formation of polycrystalline CZTSe and in agreement with earlier report [10, 23].

Effect of argon gas flow rate on deposited film structure was studied using XRD. Figure 2 shows XRD diffraction patterns for JCPDS reference, ITO/glass substrate, together with films deposited under different argon gas flow rates. The XRD pattern recorded for the deposited films, prepared from CZTSe powder under various argon gas flow rates are shown in Figures 2e-h. The

prominent Bragg reflection occurred at or around 2θ = 27.5°, especially for films prepared under 5 cm^3/min and 10 cm^3/min.

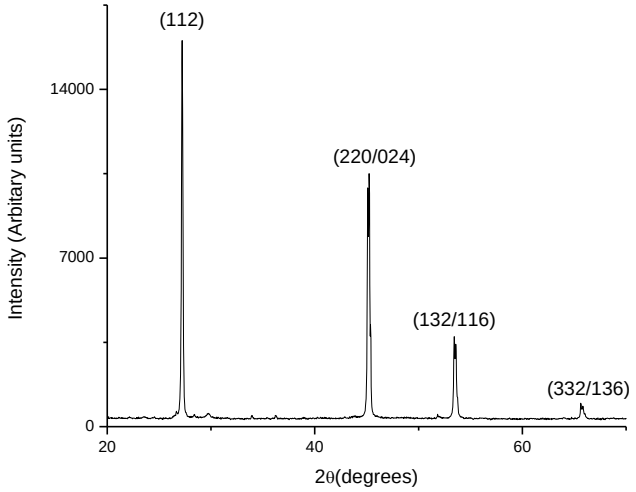

Figure 1. XRD pattern of synthesized CZTSe powder.

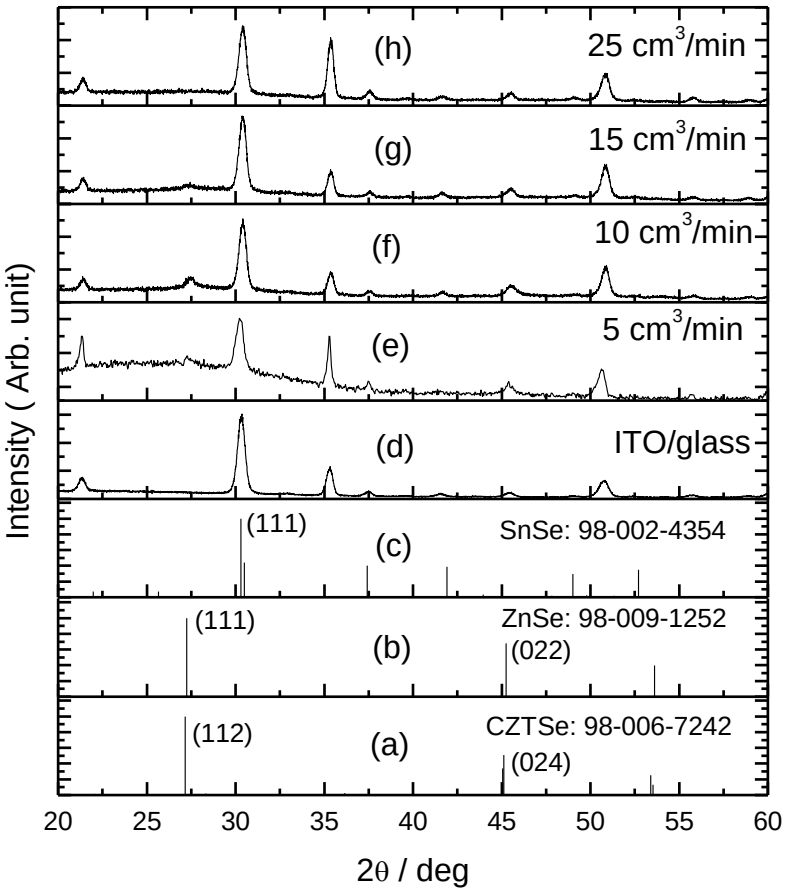

Figure 2. X-Ray diffraction spectra of JCPDS references, ITO/glass substrates and films deposited under different argon gas flow rates (V_A): (e) 5, (f) 10, (g) 15, (h) 25 cm^3/min

Based on JCPDS reference data, the deposited film peaks coincided with the typical peaks for CZTSe (Figure 2a) and ZnSe (Figure 2b) compounds. Thus, XRD analysis does not allow distinction between CZTSe and ZnSe phases. Based on the XRD patterns, Figure 2e-f, it is likely that the films may involve CZTSe and ZnSe or a mixture of the two compounds. The presence of other compounds in the films cannot be ruled out. In other cases of quaternary metal chalcogenide, Kheraj [24] experienced difficulty to distinguish between copper zinc tin sulfide and zinc sulfide phases as the two compounds coincided in their XRD peaks. XRD data were definitely supportive but not conclusive.

The broad hump in the range between 2θ = 22° - 35° in the background for films deposited under (V_A = 5 – 25 cm^3/min) in Figures 2e-h indicates that the films contained multiphases of CZTSe and ZnSe and amorphous. As argon flow rate was increased to V_A = 15 cm^3/min and above, Figures 2g – 2h show that the peak at or around 2θ = 27.5° gradually disappeared. Based on XRD patterns in Figures 2g-h, the films presumably involved SnSe compound (Figure 2c) because SnSe prominent (111) plane peak overlaps the ITO peak at or around 2θ = 30.5° matches. To further confirm whether the films involved one or two compounds, the PEC study was conducted as described below. Distinction can be performed easily as CZTSe [14] and ZnSe [25] have different types of conductivity, that is p-type and n-type respectively.

3.2 Scanning electron microscopy

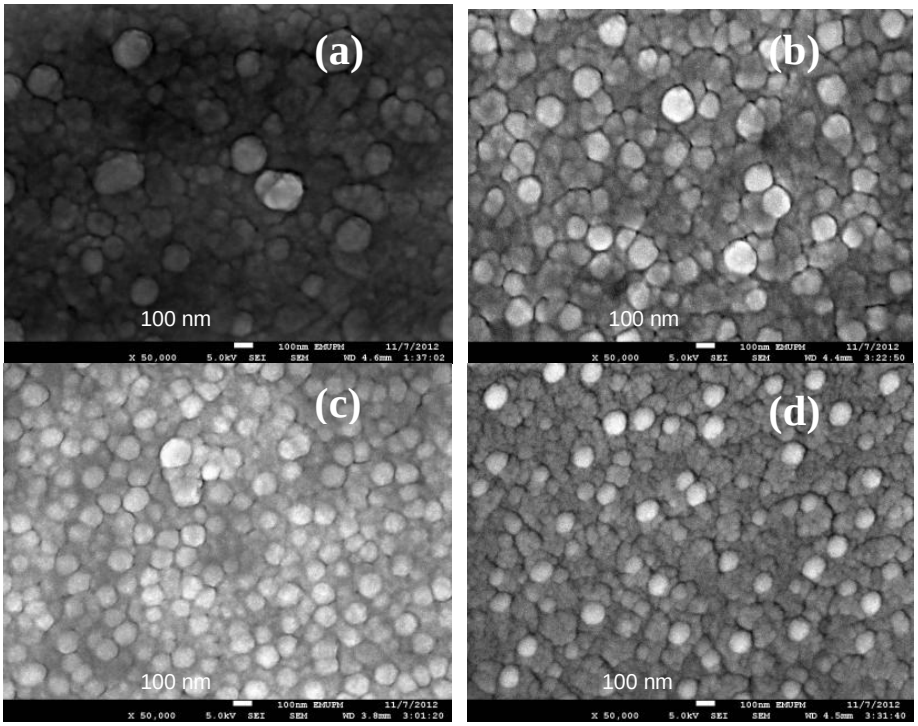

Figure 3. Surface morphology of CZTSe thin films.deposited under different argon gas flow rates (a) 5, (b) 10, (c) 15 and (d) 25 cm^3/min. Scale bars are 100 nm

Effect of argon gas flow rate on surface morphology was studied using SEM. Figure 3 shows SEM images for films deposited under different argon gas flow rates. It is evident that the deposited film grain shape and size vary by changing argon gas flow rate. The films deposited under 5 cm^3/min and 10 cm^3/min show agglomerations with irregular particle sizes as shown in Figures 3a-b. At flow rates V_A= 15 cm^3/min and 25 cm^3/min, agglomerates with more uniform shapes and smaller particles were observed. Irregular round shapes were observed for films deposited under V_A = 5 -10 cm^3/min, whereas more uniform round shapes were observed for films deposited under V_A = 15 – 25 cm^3/min.

Based on profilometry, the film thickness varied depending on the argon gas flow rate. The thickness values for films deposited under V_A = 5, 10, 15 and 25 cm^3/min were 184.0, 165.8, 197.6 and 70.0 nm respectively.

3.3 Energy Dispersive X-Ray

Table 1a shows values of average atomic % together with standard deviations measured for films prepared under different argon gas flow rates. Table 1b correlates between values of atomic % ratio and PEC characteristics for these films. The atomic % data were analyzed by area scanning (1μm X 1μm) for 5 different areas on each film. Tables 1a shows significant lowering in copper content could be clearly observed for films deposited under V_A = 15 cm^3/min and above, compared with films deposited under V_A = 5 - 10 cm^3/min; on the other hand significant enlarging in tin content could be observed.

Table 1a. Values of average and Std. Dev. of atomic % for each element in films deposited under different argon flow rates

Flow rate (cm^3/min)	Atomic % (Ave. of 5 points)				Standard deviation (5 points)			
	Cu	Zn	Sn	Se	Cu	Zn	Sn	Se
5	11.87	9.36	17.65	61.12	0.38	0.63	0.59	0.81
10	10.70	8.78	18.19	62.32	0.42	0.36	0.35	0.24
15	8.98	9.40	19.65	61.98	0.27	0.55	0.26	0.36
25	4.50	9.56	24.18	61.77	0.96	0.65	1.05	1.14

Table 1b. Atomic % ratio and PEC characteristics for films deposited under different argon gas flow rates

Flow rate (cm^3/min)	Atomic % ratio			Notes
	Zn/Se	Cu/[Zn+Sn]	Se/[Cu+Zn+Sn]	
5	0.153	0.439	1.572	n- and p- type behavior observed
10	0.141	0.397	1.654	n- and p-type behavior observed
15	0.152	0.309	1.630	p-type behavior observed
25	0.155	0.133	1.616	p-type behavior observed

The significant variation in copper and tin content indicates that the film compound changed into a new phase. Significant change of copper and tin content for films deposited under V_A = 15 - 25 cm^3/min is consistent with XRD and surface morphology results. The gradual cessation of the peak at or around 2θ = 27.5° for films deposited under V_A = 15 - 25 cm^3/min was due lowering in content of copper compounds from CZTSe. The film changed to more of SnSe phase. Such copper lowering and tin enlarging affected the structure and surface morphology, as shown in Figures 2g-h and Figures 3c-d.

3.4 Photoresponse

PEC measurement was used to study the effect of argon gas flow rate on film conduction type and to estimate PEC photosensitivity. This is necessary as the films are expected to be semiconductors, and should be sensitive to photons with energy higher than its E_g, by showing a photocurrent in the region corresponding to their minority carrier current flow. Figure 4 shows the PEC photoresponse with chopped light illumination under a linearly increased bias. Current changed (increase/decrease) when the illumination was chopped (on and off) under cathodic bias (from 0 to -1V vs Ag/AgCl) and under anodic bias (from 0 to +1V vs Ag/AgCl). Carriers are excited in the illumination region within the thin film and the excited minority carriers diffuse to the surface during their lifetime to participate in an electrochemical reaction at the film/electrolyte interface.

Figures 4(a)-(b) show that the film electrodes prepared under V_A = 5 - 10 cm^3/min exhibit positive photocurrent at voltages more positive than +0.5 V, and negative photocurrents at voltages more negative than -0.2 V. Positive and negative photocurrents exhibited by the electrodes indicate that either the electrons or the holes could be the majority carriers depending on the active material. This indicates a mixture of n- and p-type behaviors for films prepared under V_A = 5 - 10 cm^3/min. When the V_A was increased to V_A = 15 - 25 cm^3/min (Figures 4c-d), the film electrodes dominantly exhibited negative photocurrents at voltages less negative than -0.2 V, indicating a p-type behavior. Mixed n-p type behaviors for films deposited under V_A = 5 - 10 cm^3/min suggest that the films involved two types of compounds, namely CZTSe and ZnSe. The fact that CZTSe exhibits p-type conductivity and ZnSe exhibits n-type conductivity justifies the observation of both n- and p-type behaviors together. The PEC results are consistent with observed XRD patterns and reference data. Since the cathodic dark current behaviors of Figs. 4c and 4d are different from those of Figs. 4a and 4b, p-type behavior for films deposited under V_A = 15 - 25 cm^3/min indicates the presence of p-type SnSe compound not p-CZTSe. A mixture of n-p type behaviors was reported by Ghamarian [26], where impurity of Cu or Se penetrated into the prepared $CuInSe_2$ film during heat treatment. Other phenomena of mixed n-p type behaviors in PEC were also reported by Sahdan et al. [21], for In_xSn_yS thin films doped with indium. The mixed p-n type behavior was due to the material changing from p- to n-type when indium increased gradually.

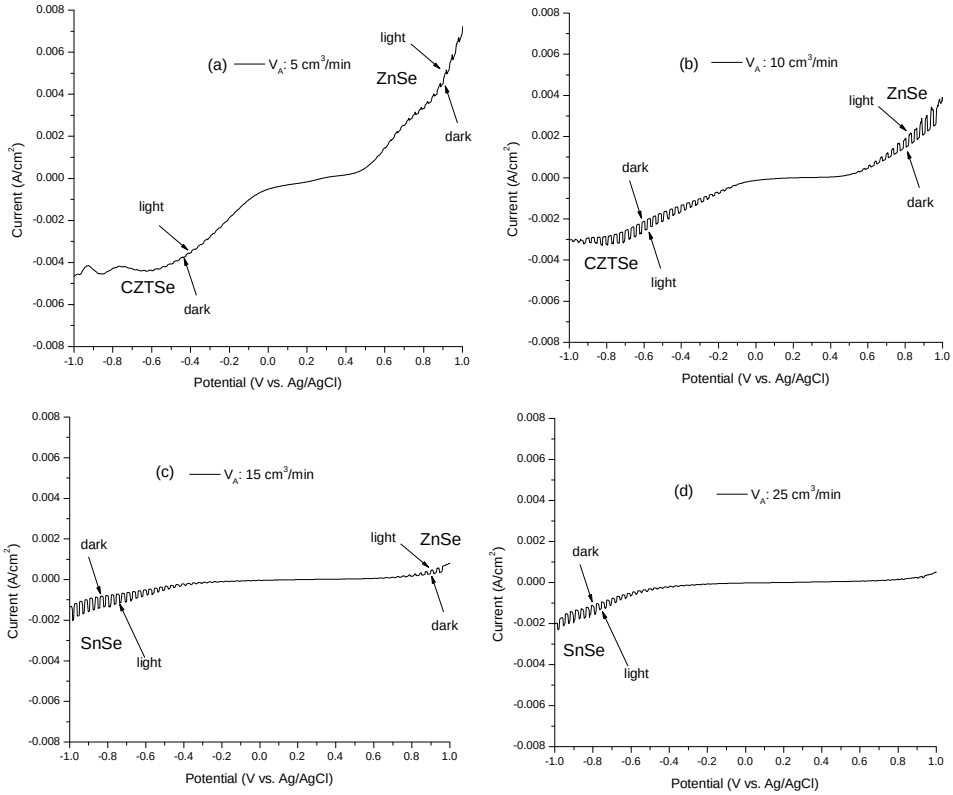

Figure 4. The PEC characteristics measured for films deposited under different argon gas flow rates (a) 5, (b) 10, (c) 15, and (d) 25 cm^3/min

3.5 Optical Properties and Band Gap Energy

Figure 5 shows absorption coefficient versus wavelength plots, obtained from UV-visible spectra, for films prepared under various argon gas flow rates. The figure shows a pronounced absorption between wavelengths of 400 and 800 nm. This indicates that all films are active in the visible portion of the spectrum and could potentially be employed as visible light energy conversion materials. To determine the band gap energy (E_g) and the transition type of the semiconductor, the optical data were treated with the Stern equation by plotting the $(\alpha h\nu)^{2/n}$ versus hν, where n=4 for indirect transition materials and n=1 for direct transition [27]. The obtained graphs with an extrapolation line to the x-axis are shown in Figure 6a-b. By extrapolating, the band gap energy values were obtained. Indirect band gap energy values estimated for film electrodes deposited under V_A = 15 – 25 cm^3/min were in the range of 1.04 and 1.13 eV, Fig. 6b. Literature shows that the SnSe film has an indirect band gap of 1.25 eV [28]. Measured band gap values indicate that the film involved SnSe compound. Indirect band gap energy values estimated for film electrodes deposited under V_A = 5 - 10 cm^3/min were 0.75 eV (Figure 6b) and direct band gap energy values estimated for film electrodes deposited under V_A = 5 - 10 cm^3/min were in the range 1.91 and 1.96 eV (Figure 6a). Ahn et al. reported that films involving CZTSe mixed with ZnSe should exhibit direct band gap values in the range 0.99 to 1.96 eV and a direct band gap value 1.96 eV was observed for a film involving CZTSe and ZnSe, deposited at substrate temperature of 430°C [29]. The fact that the estimated direct band gap

values are within the reported range, indicates that the films involved mixtures of CZTSe and ZnSe. Combined results of XRD, EDX, photoresponses and optical properties of the films provide compelling evidence in favor of formation of mixed phases, by changing argon gas flow rate. This highlights the potential value of preparing films with different mixed phases by changing the argon gas flow rate.

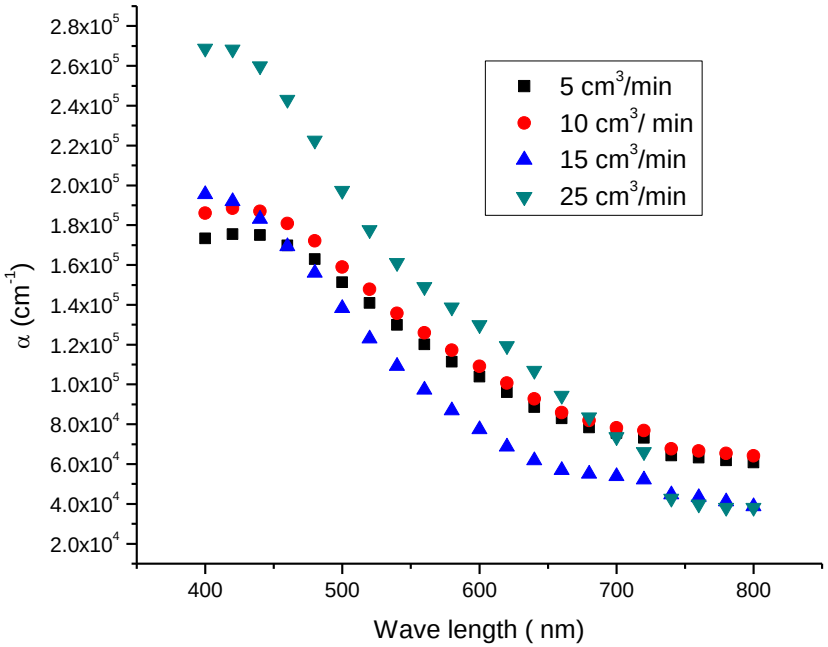

Figure 5. Absorption coefficient vs. wavelength plots for films deposited on ITO/glass under different argon gas flow rates (a) 5, (b) 10, (c) 15, and (d) 25 cm^3/min

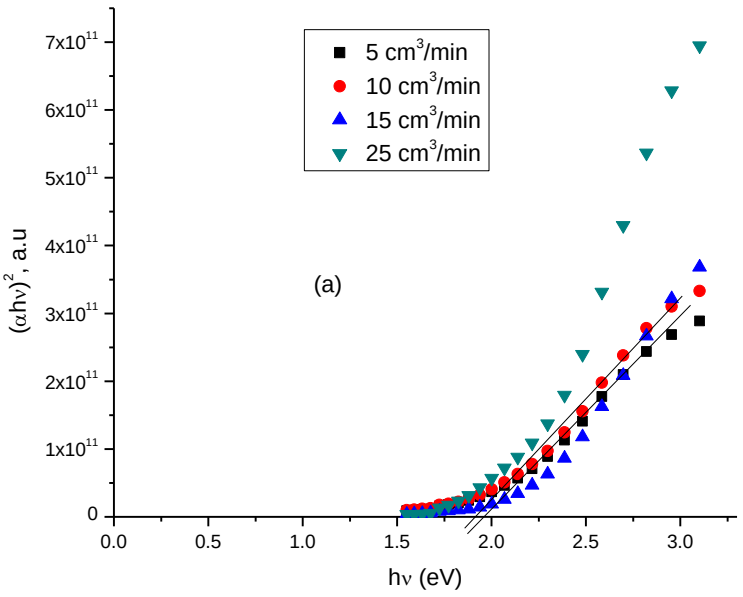

A

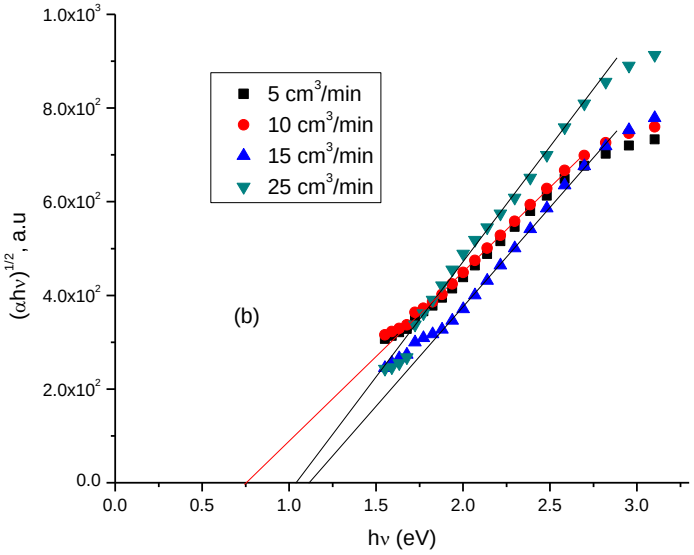

B

Figure 6. Plot of $(\alpha h\nu)^{2/n}$ vs : (a) n=1 and (b) n=4 for samples electrodes prepared under different gas flow rates

4. CONCLUSION

Film electrodes prepared by thermal vacuum evaporation from CZTSe source under various argon gas flow rates, have been successfully deposited on ITO/glass substrates for the first time. The type of electrical charge carriers for the films could be easily changed by changing the argon gas flow rate. XRD, SEM, EDX, optical and PEC test analysis indicate that the films prepared under lower argon gas flow rates is a mixed compound of CZTSe and ZnSe with different conductivity types. Films prepared under higher flow rates were found to have a single phase SnSe. The films exhibited absorption coefficient value (> 4.0 x 10^4 cm^{-1}) in the wavelength range 400 and 800 nm, showing their applicability as visible light energy conversion materials. By varying argon gas flow rate, the film conductivity could be changed from n-type to p-type or vice versa. This offers an option with easily controllable parameters that could be further applied in preparing other metal chalcogenide quaternary materials.

ACKNOWLEDGEMENT
Financial received from the Ministry of Higher Education under Exploratory Research Grant Scheme Grant No. 5527051 and UPM Research Grant Scheme is acknowledged.

References

1. R. K. Pandey, S. Mishra, S. Tiwari, P. Sahu, B. P. Chandra, *Solar Energy Materials & Solar Cells* 60 (2000) 59-72
2. R. Indirajith, T. P. Srinivasan, K. Ramamurthi, R. Gopalakrishnan, *Current Applied Physics* 10 (2010) 1402-106
3. K. J. John, B. Pradeep, E. Mathai, *Journal of Materials Science* 29 (1994) 1581-1583

4. L. Amaraj, M. Jayachandran, C. S. Anjeeviraja, *Materials Research Bulletin* 39 (2004) 2193-2201
5. P. A. Chate, P. P. Hankare, D. J. Sathe, *Journal of Alloys of Compounds* 505 (2010) 140-143
6. H. S. Hilal, R. M. A. Ismail, A. El-Hamouz, A. Zyoud, I. Saadeddin, *Electromica Acta* 54 (2009) 3433-3440
7. M. A. S. M. Yunos, Z. A. Talib, W. M. M. Yunus, M. Y. M. Sulaiman, J. L. Y. Chyi, W. S. Paulus, *Jurnal Sains Nuklear Malaysia*, 23 (2011) 46-52
8. M. Fujii, T. Kawai, S. Kawai, *Solar Energy Materials* 18 (1988) 23-35
9. C. C. Koch, Nanostructured Materials: Processing, Properties and Applications, second ed., William Andrew, Inc, Norwich, NY, 2007, 47-90
10. N. Sabli, Z. A. Talib, W. M. M. Yunus, Z. Zainal, H.S. Hilal, M. Fujii, *Materials Science Forum* 756 (2013) 273-280
11. S. Hong, C. Kim, S. Park, I. Rhee, D. Kim, J. Kang, *Molecular Crystals and Liquid Crystals* 565 (2012) 147-152
12. W. Haas, T. Rath, A. Pein, J. Rattenberger, *Chemical Communication* 47 (2011) 2050-2052
13. R. A. Wibowo, W. H. Jung, K. H. Kim, *Journal of Physics and Chemistry of Solids* 71 (2010) 1702-1706
14. R. A. Wibowo, W. S. Kim, E. S. Lee, B. Munir, K. H. Kim, *Journal of Physics and Chemistry of Solids* 68 (2007) 1908-1913
15. M. A. Contreras, B. Egaas, K. Ramanathan, J. Hiltner, A. Swartzlander, *Progress in Photovoltaic: Research and Applications* 7 (1999) 311-316
16. K. Ramanathan, M. A. Contreras, C. L. Perkins, S. Asher, F. S. Hasoon, J. Keane, D. Young, M. Romero, W. Metzger, R. Noufi, J. Ward, A. Duda, *Progress in Photovoltaic: Research and Applications* 11 (2003) 225-230
17. M. Oztas, M. Bedir, O. F. Bakkaloglu, R. Ormanci, *Acta Physica Polonica* A 107 (205) 525-534
18. A. Walsh, S. Chen, S. Wei, X. Gong, *Advanced Energy Materials* 2 (2012) 400-409
19. A. Zunger, S. B. Zhang, S. Wei, Revisiting the defect physics in $CuInSe_2$ and $CuGaSe_2$, Photovoltaic Specialists Conference, Conference Record of the Twenty-Sixth IEEE, (1997) 313-318
20. H. F. Myers, C. H. Champness, I. Shih, M. Sutton, Photovoltaic Specialists Conference, Conference Record of the Thirty-Seven IEEE, (2011) 420-424
21. M. Z. Sahdan, J. J. M. Vequizo, A. M. A. Haleem, M. Rusop, M. Ichimura, International Conference Photonics, IEEE 2nd International Conference, (2011) 1-5
22. K. S. V. Santhanam, M. Sharon, Photoelectrochemical Solar Cells, Elsevier Science, Inc, New York, NY, 1988, 156-177
23. A. Nagaoka, K. Yoshino, H. Taniguchi, T. Taniyama, H. Miyake, *Journal of Crystal Growth* 354-1 (2012) 147-151
24. V. Kheraj, K. K. Patel, S. J. Patel, D. V. Shah, *Journal of Crystal Growth* 362 (2013) 174-177
25. P. P. Hankare, P. A. Chate, S. D. Delekar, M. R. Asabe, I. S. Mulla, *Journal of Physics and Chemistry of Solids* 67 (2006) 2310-2315
26. N. Ghamarian, Z. Zainal, M. Zidan, W. T. Tan, *International Journal of Electrochemical Science*, 8 (2013) 312-322
27. F. Stern, *Solid State Physics* 15 (1963) 299-408
28. Z. Zainal, S. Nagalingam, A. Kassim, M. Z. Hussein, W. M. M. Yunus, *Materials Science* 21 (2003) 225-233
29. S. Ahn, S. Jung, J. Gwak, A. Cho, K. Shin, K. Yoon, D. Park, H. Cheong, J. H. Yun, *Applied Physics Letters* 97 (2010) 0219051-02190513